

Assembly and Test-Induced Distortions of the FUSE Mirrors – Lessons Learned

Raymond G. Ohl,^{a,b} Robert H. Barkhouser,^a Michael J. Kennedy,^c and Scott D. Friedman,^a

^aCenter for Astrophysical Sciences, Department of Physics and Astronomy,

The Johns Hopkins University, Baltimore, MD 21218

^bAstronomy Department, University of Virginia,

P.O. Box 3818, Charlottesville, VA 22903

^cThe Johns Hopkins University Applied Physics Laboratory, Laurel, MD 20723

ABSTRACT

The Far Ultraviolet Spectroscopic Explorer (FUSE), currently undergoing integration and scheduled for a 1998 launch, is an astrophysics satellite designed to provide high spectral resolving power ($\lambda/\Delta\lambda = 24,000\text{--}30,000$) over the interval 905–1187 Å. It consists of four normal incidence primary mirrors which illuminate separate Rowland circle spectrograph channels equipped with holographic gratings and delay line microchannel plate detectors.

The mirrors are fabricated from Zerodur blanks, which were 70% lightweighted and then figured to off-axis parabolas with $\lambda/40$ RMS surface figure errors ($\lambda = 6328$ Å). Each mirror is mounted to its own composite sandwich plate, which serves as a bed for heaters and also isolates the mirror from forces and moments induced by the tip/tilt/focus actuators. A flight-like qualification unit is built up in order to verify that the mirror maintains an acceptable optical figure after assembly and environmental testing.

Unexpected optical distortions during assembly and environmental testing of the qualification unit resulted in substantial modifications to the assembly procedure, as well as alteration of component and satellite thermal test limits. Known or suspected sources of distortion which warranted investigation included: assembly-induced strain, thermal relaxation of the mirror flexure adhesive, changes in the moisture content of the composite plate facesheets, and warpage of the composite plate with initial thermal cycling. This paper describes how these problems were diagnosed and addressed in order to provide mirrors meeting the optical performance requirements of the FUSE program.

Keywords: FUSE, ultraviolet, off-axis parabola, composite, actuator, flexure, lightweighted, optical testing

1. INTRODUCTION

The Far Ultraviolet Spectroscopic Explorer (FUSE) is a NASA astrophysics mission designed to produce high resolution spectra ($\lambda/\Delta\lambda = 24,000\text{--}30,000$) over the 905–1187 Å region, to address fundamental questions related to the origin and evolution of the universe.

The spectral window to be opened by FUSE will permit the study of many important atoms, ions, and molecules which cannot be investigated with other satellites. This wavelength range is extremely rich in spectral absorption lines arising within interstellar gas, the material from which stars and planets form. The far ultraviolet range also provides an opportunity to answer important questions about many types of objects, such as quasars, massive stars, supernovae, planetary nebulae, and the outer atmospheres of cool stars and planets. FUSE will measure the abundance of deuterium, an isotope of hydrogen, in a variety of astrophysical environments from the local interstellar medium to distant clouds along the lines of sight toward quasars and active galactic nuclei. These measurements will determine the extent to which stellar processing has modified the primordial abundance of deuterium, thereby

Other author information:

R.G.O.: E-mail: ohl@pha.jhu.edu

R.H.B.: E-mail: rhb@pha.jhu.edu

M.J.K.: E-mail: kennedy@pha.jhu.edu

S.D.F.: E-mail: scott@pha.jhu.edu

providing a better understanding of the amount produced in the Big Bang and the subsequent chemical evolution of the universe.

FUSE will also make significant contributions to many other areas of astronomy. Among these are the measurement of interstellar O VI absorption and determinations of the properties of hot gas in the Milky Way and Magellanic Clouds; searches for the observational signature of the hot intergalactic medium, to determine how the universe evolved at high redshifts; and measurements of molecular hydrogen, the primary constituent of the cold interstellar medium, from which protostars and their planetary systems form.

The instrument consists of four normal incidence, off-axis parabolic mirrors of 2245 mm focal length, which are co-aligned and illuminate separate 1652 mm diameter Rowland circle spectrograph channels with holographically ruled spherical gratings (see Fig. 1).^{1,2} A pair of spectra fall on each of two microchannel plate detectors with delay line anodes.³

The instrument structure is composed of a graphite/cyanate ester composite material with a coefficient of thermal expansion (CTE) of $0.0 \pm 1.08 \times 10^{-6} \text{ in/in/}^\circ \text{ C}$, designed to ensure dimensional stability over long (~ 200 kilo-second) integrations. However, mechanical G-release, thermal expansion, and moisture desorption are expected to change the structure significantly upon orbital insertion and over the life of the satellite. Each mirror is therefore equipped with precision actuators that permit independent tip, tilt, and focus control for on-orbit alignment.

In this paper we review the design of the FUSE mirror assemblies⁴ and discuss our experience during the qualification and execution of the mirror assembly plan, including a summary of problems encountered, their diagnosis, and subsequent mitigating action. In conclusion, we summarize the “lessons learned” thus far from the FUSE primary mirror assembly and test program.

2. OPTICAL DESIGN

The FUSE optical path begins with four independent, co-aligned primary telescope mirrors. Each mirror is an off-axis parabola with a rectangular aperture measuring 387.0×351.8 mm and a focal length of 2245 mm. The four mirror substrates are identical, with the proper off-axis section set by an aperture stop located near each

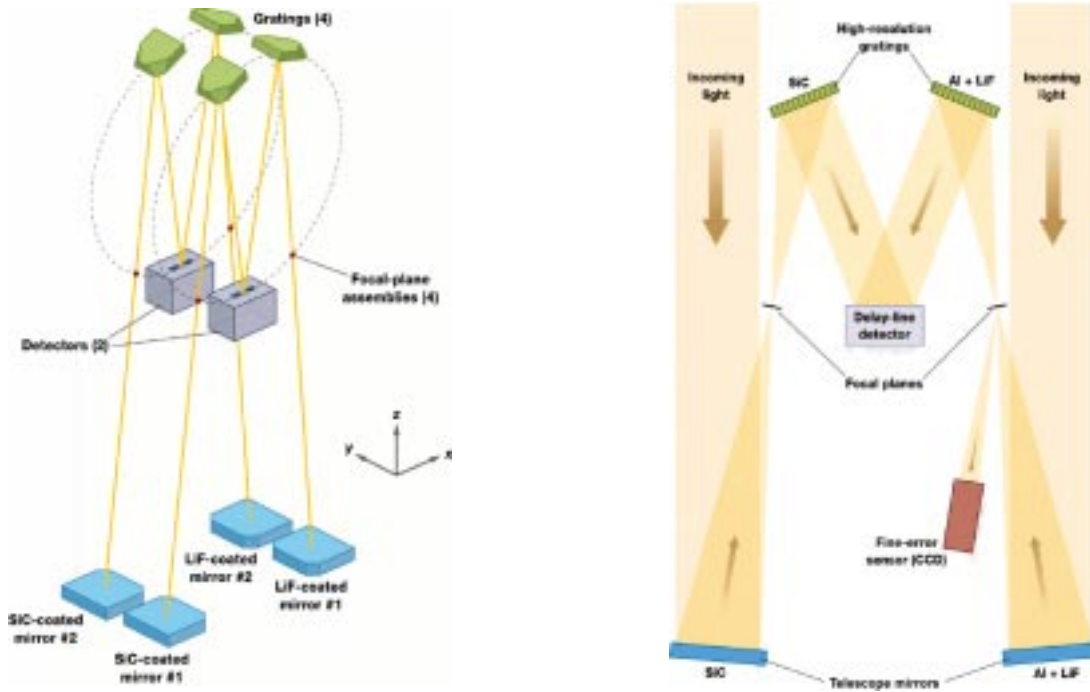


Figure 1. (a) Schematic diagram of FUSE optical design baseline. (b) Cartoon showing collimated light entering one side of the FUSE instrument (two optical paths, one detector).

mirror surface (slightly different off-axis sections are dictated by the grating incidence angles required to optimize the spectrograph channels for two wavelength bands). The two inside corners of each mirror are masked to match the grating apertures, which are missing the outside corners due to space constraints. The resulting geometric area of each mirror is approximately 1330 cm². The apertures are widely separated on the instrument optical bench, resulting in four parallel and separated optical axes. Alignment flats located on three sides of each substrate allow mirror optical axes to be aligned with the rest of the instrument during integration.

The FUSE mirrors must perform to stringent optical requirements. For an on-axis point source, 90% of the energy at 1000 Å must be within a diameter of 1.5 arcsec, which corresponds to a 16 μm diameter at the focal plane. A Gaussian image distribution satisfying this requirement has a full width at half maximum of 0.8 arcsec. Such performance is necessary to insure adequate throughput through the 1.25 arcsecond, high-resolution spectrograph slit. A secondary consideration is the spectral resolution achieved when using wider slits, in which case the imaging performance of the mirrors could limit the resolving power of the instrument. In order to meet the image size requirement, tight fabrication tolerances were established based on initial performance predictions carried out at the Johns Hopkins University (JHU) and on specifications of other far ultraviolet mirrors, such as those in the SUMER instrument on SOHO. The surface specifications are as follows: figure error better than λ/40 RMS and λ/10 peak-to-valley (P-V) at λ = 6328 Å; midfrequency error less than 20 Å RMS over 0.1–10.0 mm spatial scales; microroughness less than 10 Å RMS. These specifications have been verified by an independent analysis⁵ using the Optical Surface Analysis Code, which predicted 92% encircled energy within a 1.5 arcsecond diameter, but with a bright core containing 85% of the energy within only 0.5 arcsecond. The fabrication tolerances are challenging given the aperture configuration and the aggressive lightweighting of the mirror blanks. Figure testing, measurements of surface roughness, and preliminary image data indicate that the FUSE flight mirrors meet their performance requirements.

Two different optical coatings are employed to maximize the reflectivity of the mirrors for two wavelength bands. Two channels operate over 905–1100 Å, and the mirrors for these channels have been coated with ion beam sputtered silicon carbide (SiC) over an evaporated aluminum layer. The aluminum layer lowers the emissivity of the surface for better thermal control. The remaining two channels operate over 980–1187 Å, and these mirrors are coated with lithium fluoride (LiF) over aluminum. SiC has a nearly constant reflectivity (≈ 30%) over the FUSE bandpass. The reflectivity of Al+LiF is low shortward of ≈ 1025 Å, above which it rises sharply to ≈ 70% near 1200 Å. All of the coatings for the FUSE mirrors have been applied by the Optical Thin Film Laboratory at the Goddard Space Flight Center (GSFC).

The two LiF mirrors will also supply visible light images over a 21 arcminute field to the Fine Error Sensors, which are used for target acquisition and fine pointing control (see Fig. 1b). These sensors operate over 4000–9000 Å, where the Al+LiF reflectivity is expected to vary between 85–90%.⁶

A major concern with Al+LiF coatings is the rapid loss in UV reflectivity with exposure to atmospheric water vapor. A great deal of effort is going toward limiting to less than 100 hours the total exposure of the LiF coatings to a non-purged environment. Whenever possible, the mirrors have been under a continuous nitrogen purge. Allowances for significant degradation (20% for LiF and 15% for SiC) from the expected initial reflectivities have been incorporated into the effective area budget for the instrument. These allowances are based on data from previous programs including Copernicus,⁷ the Hopkins Ultraviolet Telescope, and the long-standing JHU sounding rocket program.⁸ In addition, LiF aging studies are currently underway at GSFC and JHU in an effort to better understand the exposure limits required to maintain high reflectivity in the UV.

3. MECHANICAL DESIGN AND BASELINE ASSEMBLY AND TEST PROCEDURE

The components of a FUSE mirror assembly are shown in Fig. 2.⁴ The actuator assembly mounts to the instrument optical bench via a three-point interface with manual adjustment for ground alignment. Three axial post flexures, which support the upper assembly in piston, are co-axial with the actuator ball screws and connect them to the composite intermediate plate (IP). Three additional, lateral post flexures secure the upper assembly in the plane perpendicular to the optical axis. The IP primarily isolates the mirror from moments that can be induced by adjustments of the actuators. The mirror is attached to the IP via three blade flexures, oriented with soft axes radial to the center of the mirror (i.e. with strong axes tangential to a circle centered on the mirror). A rectangular “pie pan” rigidly attaches to the IP. The pie pan and IP enclose the mirror on 5 sides. An aluminum aperture stop, painted with Lord Corp.’s Chemglaze Z306, is fixed to the top rim of the pie pan.

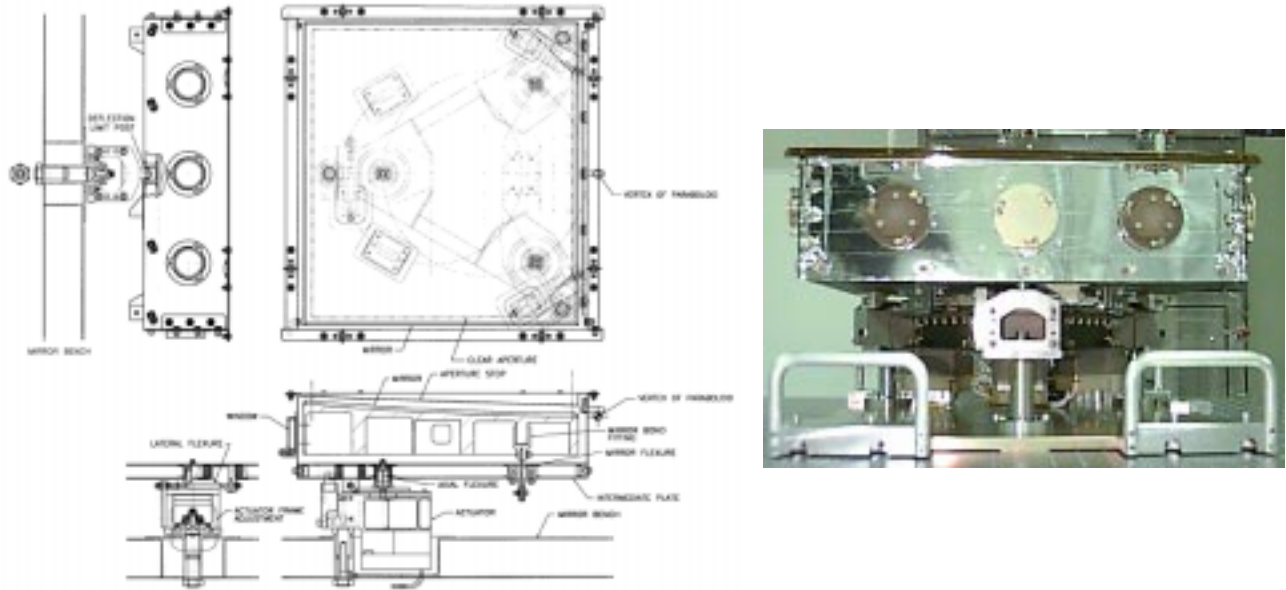


Figure 2. (a) Mirror assembly configuration. (b) Photograph showing anti-vertex side of completed FUSE mirror assembly mounted for transport on handling plate.

3.1. Design and Assembly Procedure

The four mirror substrates are fabricated from Zerodur, which was chosen for its low CTE. The mirrors are 70% lightweighted with a triangular isogrid rib pattern (see Fig. 3), leaving a 7.5 mm-thick face sheet, and weigh ≈ 17 lb. each.

The mirror flexures consist of 6Al-4V titanium alloy blades attached to Invar fittings with Hi Lok fasteners. After mirror substrate fabrication, the low-CTE Invar fittings are bonded to the mirror ribs with Hysol EA 9396 adhesive, which is allowed to cure at room temperature for several days (see Fig. 3).

The optical surface is then coated at room temperature. For Al+SiC and Al+LiF, the mirror is under vacuum for ≈ 12 and ≈ 5 days and the combined coatings are ≈ 750 and ≈ 650 Å thick, respectively.

After coating, the mirror assembly build-up begins with the mirror supported face-down on its four corners. The IP is attached to the mirror using two titanium right-angle clips which sandwich each flexure blade and mate to aluminum inserts bonded into the IP. The clips are secured with screws and subsequently match drilled and pinned through the flexure blade and into the IP inserts. In addition to providing for the CTE differences between the mirror and IP, the blade flexures on the mirror allow for slight misalignment errors in the compliant axis when the mirror is attached to the IP during assembly (0.001 in per flexure).

The composite IPs are designed for a high stiffness-to-weight ratio and to match the thermal expansion properties of the instrument structure. Each IP consists of two facesheets bonded to a core of vented Al honeycomb with FM-73 film adhesive. Each facesheet is made of 16 plies of 0.0025 in-thick M55J/9542A graphite/cyanate ester prepreg with $CTE = 0.0 \pm 1.08 \times 10^{-6}$ in/in/ $^{\circ}$ C. The mirror assembly's strip heater is mounted on the mirror-side of the IP and keeps the assembly at $22 \pm 5^{\circ}$ C, minimizing thermal distortions of the assembly components.

The mirror and IP sub-assembly is then rotated face-up and lowered onto the actuator assembly. The axial post flexures fit through additional inserts in the IP and are secured on the mirror side of the IP with nuts. They constrain the upper assembly in three degrees of freedom: translationally along the optical axis and rotationally about the axes that define the plane perpendicular to the optical axis. The titanium lateral flexures connect the actuator assembly to the IP via brackets on the actuator housings and on inserts in the IP. They lie in the plane perpendicular to the optical axis and therefore stiffen the assembly in the remaining three degrees of freedom. The actuators have sub-micron resolution and will allow ground controllers to move the mirrors in tip, tilt, and focus for

any re-alignment necessary to adjust the telescope to the post-launch environment and to accommodate structural changes over the life of the instrument.

Lastly, the pie pan is attached to the edge of the IP, stiffening it and providing an enclosed purge volume when the protective lexan mirror cover is installed. The pie pan is designed such that its CTE matches that of the IP and the inner sides, facing the mirror substrate, have a lower emissivity than the etched Zerodur, thereby minimizing heat transfer to and from the sides of the mirror.

3.2. Optical, Mechanical, and Thermal Testing

Optical figure testing is performed at each stage of the assembly process, as well as prior and subsequent to vibration and thermal-vacuum tests. Mirror figure is also monitored as a function of actuator movement. A He-Ne (6328 Å) laser unequal path interferometer (LUPI)⁹ is used to develop a surface map of the test optic. The optical test setup is shown schematically in Fig. 4a. The focus of the beam diverger (mounted in front of the LUPI) is located at the focal point of the mirror. The beam is collimated by the parabolic mirror and returned by an auto-collimating flat mirror with $\lambda/20$ P-V surface errors at 6328 Å. The FUSE mirror under test is supported at two points in a fashion that minimizes gravitational sag and mirror assembly hardware is similarly off-loaded (see for example Fig. 4b).⁴ This system allows sampling of mirror surface structure down to $\approx \lambda/25$ P-V and is sensitive to global surface errors $> \lambda/200$ RMS. In order to meet the encircled energy requirements discussed above, a fully assembled flight mirror must have $\leq \lambda/20$ RMS surface errors.

After the mirror assembly is fully assembled and optically characterized, the unit undergoes environmental testing to simulate launch and on-orbit conditions. The vibration test takes place at the Johns Hopkins University Applied Physics Laboratory (APL) and consists of sine and random motions in three orthogonal directions.

After the vibration test, the full mirror assembly undergoes thermal-vacuum qualification and thermal balance tests (TV) at APL. The thermal environment seen by the assembly is controlled by the heaters on the mirror side of the IP in addition to heaters elsewhere in the vacuum chamber. The thermal survival limits (plus a 10° C margin) are tested by cycling the temperature from +50° C to -20° C. The extremes of assembly operating temperature (plus a 10° C margin) are tested by cycling the temperature six times from about +37° C to about +7° C.

Each part of the assembly and test procedure was qualified with an engineering test unit mirror (ETU) before any flight mirrors entered the flow. The ETU is flight-like in all respects, except it has a spherical optical surface.

4. ASSEMBLY AND QUALIFICATION PROBLEMS

This section summarizes the four independent, unforeseen challenges encountered during the mirror assembly program in chronological order of their discovery. Only those potential causes that were addressed during our program thus far are discussed here.

4.1. Initial Epoxy Cure

The first problem encountered was the first of several attributed to, and most obviously associated with, the characteristics of the adhesive, Hysol EA 9396, used to bond the Invar fittings to the mirror ribbing (see Fig. 3). ETU figure testing at SVG Tinsley, Inc.* after flexure bonding revealed the presence of a $\lambda/10$ -high “bump” in the surface of the mirror at each flexure location which was not present beforehand (see Fig. 5a). Although weak in amplitude, an additional, overall, “Y-shaped” indentation with a three-pronged symmetry manifested itself, centered on the mirror and oriented such that each branch of the “Y” was roughly centered on a flexure location (bump). Tinsley thus saw a degradation in the ETU’s overall figure error from 0.016λ RMS before, to 0.028λ RMS after flexure bonding. After delivery, the ETU’s surface error was measured at JHU to be 0.034λ RMS.

This change was well-correlated with flexure bonding and the bumps coincided exactly with the flexure locations. It was therefore immediately suspected that this figure error was strain in and/or bending of the mirror substrate caused by the epoxy upon cure. For further characterization, Tinsley fabricated a 15 cm diameter Zerodur sample with representative mirror facesheet thickness and lightweighted-pocket geometry, to which was bonded a flight-like flexure. (This sample was polished flat to $\approx \lambda/120$ RMS surface error before bonding the flexure.) After the adhesive

*Silicon Valley Group, Inc., Tinsley Division, Tinsley Laboratories, 3900 Lakeside Dr., Richmond, CA 94806-1963. Tinsley lightweighted the Zerodur blanks and figured the mirrors into paraboloids.

cured, the flat’s figure was measured to have degraded to 0.026λ RMS. The only surface feature was a $\approx \lambda/10$ -high bump centered on the flat, over the flexure location.

This problem was addressed by changing the procedure for flight mirror manufacture: Flexures were bonded prior to polishing for final figure, so any distortion the adhesive might induce would be removed (i.e. the bumps would be polished off). However, the last stage in mirror substrate fabrication is the removal of a polishing extension (lip) around the mirror edge. Figure measurements afterward showed that the flight mirrors had deformed to a Y-shaped ridge, centered on the mirror and oriented such that each branch matched up with a depression superimposed at the location of each flexure (see Fig. 5e). This Y-shape was opposite in sign to that observed initially on the ETU (i.e. inverted — compare Figures 5a and 5e). (Note that removal of the polishing extension on the ETU took place before flexure bonding and did not change the mirror figure.) Our choice of flexure epoxy not withstanding, Tinsley was able to produce flight mirrors that met delivery specification: Typical overall figure errors were $\approx 0.025\lambda$ RMS. Before lip-removal, the flight mirrors had $\approx 0.015\lambda$ – 0.020λ RMS surface errors (similar to the ETU before flexure bonding and exceeding delivery specification).

We infer that prior to final polish and lip-removal, the stress from the epoxy curing would have manifested itself as bumps above the flexures and a Y-shaped depression in the flight mirror surface (as it did in the ETU’s case, although the flexures were bonded after the ETU’s lip was removed). Removing the lip from the flight mirrors made them more flexible, allowing stress in the mirror from the cured adhesive to distort the mirror. This reduced the amount of local stress and strain in the mirror above the flexure points, producing depressions in the areas where the bumps were polished off, because the polishing extension was stiffening the mirror and keeping those three areas locally “flat.”

4.2. Post-Thermal Vacuum Test Primary Distortion

The most significant problem arose after the completed ETU mirror assembly underwent TV. Figure test data for the ETU-plus-IP sub-assembly (i.e. detached from the actuators and pie pan) before and after TV are displayed in Fig. 5b and 5c. These results indicate that the mirror distorted from an overall figure error of 0.049λ RMS before, to 0.300λ RMS after TV. The change manifested itself primarily as astigmatism. A flight mirror with this degree of figure distortion would impact both throughput and spectral resolution and would result in the loss of scientific data from the mission.

A number of issues were identified as relevant to the cause of the post-TV distortion:

1. The Hi Lok fasteners in the mirror flexure that connect the Invar fitting (epoxied to the mirror rib) to the titanium flexure blade were meant to give a slight interference fit (see Fig. 3). It was noticed during assembly that there was generally some clearance in the fit (0.0001 – 0.0002 in.). Any movement due to thermal expansion between the mirror and IP that could break friction in this fitting and put the IP and mirror into a different configuration would lock a new stress into the mirror, changing its figure.
2. The IPs contain a large amount of FM-73 and some of Hysol’s EA 9394 adhesive (around the inserts). Since the IP was stored in a non-purged environment before TV, it could have changed shape via desorption of moisture during TV from the epoxy or elsewhere in the composite IP, thereby stressing the mirror through the flexures.
3. Perhaps the heaters (mounted on the mirror side of the IP) differentially dried out one side of the IP relative to the other during TV, warping the IP and stressing the mirror. Note that the ETU IP strip heaters were never activated before TV (i.e. the strip heaters on the IP were not used to help bake-out the IP after fabrication).
4. If the EA 9396 adhesive bonding the flexures to the mirror moved or stress-relieved during TV with the change in temperature or from moisture desorption, the flexure could move relative to the mirror. When heated above its glass transition temperature (T_g), a cured adhesive becomes less rigid. EA 9396 has a different T_g when allowed to cure at different temperatures (e.g. $T_g = 77^\circ$ C when cured for 5 days at room temperature).¹⁰ While trying to shorten the length of the ETU’s TV, we briefly subjected parts of the assembly to a temperature warmer than the range described in Section 3.2: Though the mirror remained cooler than 59° C, the center of the IP did reach about 75° C. Note that the EA 9394 epoxy used to hold the inserts in the IP has properties similar to EA 9396 and could have a similar T_g .

The diagnosis of this problem proceeded along several fronts. Upon confirmation of the severe distortion, the ETU assembly was taken apart, piece-by-piece, and the mirror figure tested at each step to isolate the hardware that caused the distortion. The ETU figure improved significantly only when the IP was fully detached from the mirror (but see Section 4.3).

A series of measurements was made at Swales and Associates, Inc.[†] of IP shape as a function of moisture absorption, desorption, and pre- and post-thermal cycling. IP shape was monitored via three optical cubes, each bonded to a flexure-mounting insert. These experiments and previous modeling indicated that a dry IP stored at room temperature and at typical room humidity would progress toward saturation with typical fractional mass change $\approx 0.1\%$ /hour during the first few minutes after removal from purge, to $\approx 0.01\%$ /day days later and reach saturation on the timescale of weeks. The IPs were seen to alter shape significantly after the first time they were thermally cycled (using the IP strip heaters for the first time). No significant change in IP shape was seen afterwards, regardless of thermal environment or moisture absorption, but measurements were not accurate to less than 10 arcsec. It is unclear what effect a change smaller than this limit would have on the mirror. Point 2 above was further addressed by attaching a dry IP to the ETU (with screws only — no pins) and monitoring its figure as the IP absorbed moisture in room air over the course of 11 days. No significant change in figure was observed. The blade flexures were designed to flex radially in order to accommodate IP expansion or contraction in the plane perpendicular to the optical axis. However, they are stiff in the direction tangential to the circle on which they are located. It is likely that any IP expansion or contraction with a significant out-of-plane component (warping) could have produced a moment in the strong axis of the flexures, which would be seen as a distortion in the surface of the mirror.¹¹

In an attempt to investigate blade flexure movement from the adhesive’s dependence on temperature and/or moisture content (item 4 above), the orientations of the flexures on a flight mirror were measured before and after thermal cycling at a thermal-vacuum facility at the University of Colorado, Boulder. This test was inconclusive.

At this time it is unclear what caused the severe distortion in the ETU mirror after TV, but the following changes to the assembly procedure have greatly mitigated this effect: The Hi Lok fasteners joining the Invar fitting to the titanium flexure blade were replaced with interference-fit shear pins. Each IP was thermally cycled before assembly and baked-out dry using the TV chamber and IP strip heaters, then kept dry during the assembly process. The IP is attached to a mirror with screws only; the mirror-plus-IP sub-assembly is subjected to TV and tested before and after for satisfactory figure; the sub-assembly is then permanently pinned; finally, the actuators, which are sent through TV separately, are attached. It is anticipated that any change in mirror figure due to further IP moisture absorption during instrument-level integration and test will relax when the assembly is in the space environment, where desorption can take place. We will further investigate this effect by permanently pinning an IP to the spare flight mirror and testing it before and after TV.

4.3. Post-Thermal Vacuum Test Secondary Distortion

When the IP was removed from the ETU after TV, the mirror’s figure did not return to the value measured prior to assembly (see Figures 5a and 5d). After ensuring the proper “phasing” of our surface data, it was confirmed that the ETU’s figure had inverted from 0.034λ RMS before TV, represented as bumps at the flexure locations and an overall Y-shaped depression on the mirror, to 0.028λ RMS after TV, with the bumps superimposed on a Y-shaped ridge. The “difference map” (not shown) between these two images has 0.049λ RMS surface error and clarifies this sign reversal. Thus, a “permanent” or “residual” distortion from the mirror’s original shape remained in the mirror after all assembly hardware had been detached. This degree of distortion is much more subtle than that discussed in 4.2 (compare Figures 5c and 5d).

At this junction it had been well established that the adhesive imparts a stress to the mirror after cure (see Section 4.1). The adhesive could have changed the amount of stress it imparts to the mirror in response to a different temperature or humidity seen during TV, thus changing the mirror distortion. The symmetry of the distortion strongly supported this hypothesis.

In order to better characterize the behavior, Tinsley thermally cycled the small flat mirror with attached flexure mentioned in Section 4.1 to increasing positive temperature extremes (not in vacuum), while measuring the figure between runs (2 thermal cycles per run). Details of each thermal cycle and the resulting figure error are presented in Table 1. Qualitatively, the dominant feature on the surface of this flat was the central bump first observed after

[†]Swales and Associates, Inc., 5050 Powder Mill Rd., Beltsville, MD 20705

the flexure was bonded. The bump was seen to decrease in amplitude after the first and second cycles. After the third cycle, however, the bump was replaced by two features: a depression on one side of the flexure bondline and a matching bump on the other, each feature located over one of the lightweighted pockets that define the rib on the back of the mirror. That is, the bump and the depression gave the mirror surface an “S-shaped” profile when viewed in cross-section.

Tinsley also measured the figure of the ETU before and after thermally cycling it from -20°C to $+37^{\circ}\text{C}$. The overall figure improved from 0.028λ RMS to 0.020λ RMS. There was little change observed at the flexure locations (bumps), but the overall amplitude of the Y-shape decreased.

This problem was addressed by lowering the maximum temperature seen by the mirrors during any part of integration, test and flight from $+50^{\circ}\text{C}$ to $+40^{\circ}\text{C}$. Appropriate thermostats were added to the primary and backup heater circuits. Note that, later, two flight mirrors that had been through TV — and were figure tested for other reasons afterward without any other hardware attached — showed significant figure degradation (but see Section 4.4).

Table 1. Synopsis of Tinsley vacuum thermal cycle and figure test data for small flat sample in investigation of post-TV, secondary distortion.

	PRE-CYCLING (POST-CURE)	-20°C TO $+45^{\circ}\text{C}$	-20°C TO $+60^{\circ}\text{C}$	-20°C TO $+70^{\circ}\text{C}$
RMS	0.026λ	0.021λ	0.015λ	0.019λ
DESCRIPTION	$\approx \lambda/10$ BUMP	SMALLER BUMP	EVEN SMALLER BUMP	OFFSET BUMP & NEW DIP

4.4. Figure Change with Constant Environment

The figures of at least four of the five flight mirrors fabricated were observed to change over time during storage in a constant, room temperature, usually N_2 purged storage environment. Mirrors changed while both mounted and unmounted to other assembly hardware. Typical changes were $\sim 0.03\lambda$ RMS over time scales ranging from 2 weeks to more than 2 months (see Table 2). This behavior, confirmed by independent measurements at Tinsley, complicated the diagnoses of the effects described in Sections 4.2 and 4.3.

The most likely explanation is that the stress in the mirror from the EA 9396 adhesive along the flexure bondline depends on moisture content and the epoxy is desorbing while the mirrors sit for long periods in the dry N_2 purge. Figure tests showed that the Y-shaped distortion was changing, implicating a stress associated with the flexures. Efforts to correlate these changes more closely with mirror storage environment are currently underway.

It is possible that stress built up in the mirror substrates could be slowly relieving in a “delayed elasticity” effect,¹² distorting the mirror over time. However, this does not explain the behavior of the mirrors that improved, then later degraded, or vice versa. Also, the time scale and amplitude of the distortion expected from delayed elasticity are in great disagreement with our observations.

Lack of proper characterization of this subtle effect and reasonable options for mitigation have limited our action. The effect of moisture absorption and desorption over long time scales is being investigated: We are monitoring the figure of one mirror stored in “open air” and we are in the process of building an ETU-plus-IP sub-assembly and monitoring its figure while in storage, under purge. We continue to monitor the mirrors before integration with the FUSE instrument to ensure their figure quality exceeds the specification required to meet mission goals.

Table 2. Mirror figure change while in a constant, room-temperature storage environment.

MIRROR NAME	ASSEMBLY STATUS [‡]	STORAGE ENVIRONMENT	DATES	RMS (λ)
SiC 2 [§]	<i>M</i>	N_2	09/16/97–10/02/97	0.048–0.020
SiC 1	<i>FULL</i>	N_2	11/12/97–01/23/98	0.031–0.049
SiC 2	<i>FULL</i>	N_2	12/22/97–01/31/98	0.042–0.053
LiF 1 [¶]	<i>M, M + IP</i>	N_2	01/27/98–03/03/98	0.042–0.039
SPARE	<i>M</i>	AIR & N_2	05/12/97–02/10/98	0.025–0.050
SPARE	<i>M</i>	AIR & N_2	02/12/98–02/22/98	0.050–0.041

5. CONCLUSION AND LESSONS LEARNED

Three unanticipated problems arose during fabrication, assembly, and testing the FUSE primary mirror qualification unit that led to a revision of the baseline procedure and test specifications. The epoxy used to bond the mirror flexures distorted the mirror substrate upon cure. For the flight mirrors, bonding of the flexures was moved earlier in the fabrication process, but distortion then appeared when the polishing extension was removed. Based on its geometry, we also attribute this distortion to the epoxy. Though distorted, the mirrors met delivery specification. It was discovered after TV that the IP can stress the attached mirror, distorting it to unacceptable levels if it changes shape. Exposing the IP to TV before assembly, drying it out, keeping it dry during assembly, and changing the order of permanent pinning and TV in the procedure fully mitigated this effect. The stress in the mirror from the epoxy along the mirror-flexure bondline was found to change with exposure to a higher thermal environment. The mirror assembly survival temperature upper limit was therefore decreased to ensure a constant mirror figure. Though steps could be taken to address these three problems, an on-going investigation is seeking to characterize and look for correlations with the subtle changes in mirror figures as they sit in storage.

The most important lesson to draw at this time from our experience with the FUSE mirror assembly and test program is that the prudent course is to thoroughly test and understand how materials behave in every relevant environment and on a level that is meaningful to mission performance. In our case, though EA 9396 has excellent strength characteristics, the impact of the flexure epoxy on the lightweighted optics was not fully characterized before mirror fabrication for the environments expected during integration and test and on-orbit, nor was it completely understood when problems arose during fabrication of the ETU. However, the post-TV distortion associated with the IP was fully tractable with variations on our planned assembly and test procedure, but cost and schedule constraints prevented us from obtaining a complete picture of the behavior. The entire FUSE mirror team worked hard and reacted quickly to these challenging problems. Our limited investigation notwithstanding, we have produced mirror assemblies that meet or exceed the performance requirements for the FUSE mission.

For more information about the mission, see the FUSE web homepage at: <http://fuse.pha.jhu.edu>.

[‡]*M* = mirror alone, *M + IP* = mirror with intermediate plate attached, *FULL* = full mirror assembly

[§]Initial measurement made after mirror was thermally cycled alone.

[¶]The first measurement is the mirror alone after TV, while the second measurement was taken after an IP was added, the sub-assembly sent to TV, and finally drilled and pinned permanently together. Although the change is only a small improvement, it probably reflects an improving mirror substrate, as adding an IP, going through TV, drilling holes and pinning caused the other mirrors to degrade.

^{||}This mirror never experienced a temperature environment warmer than room temperature.

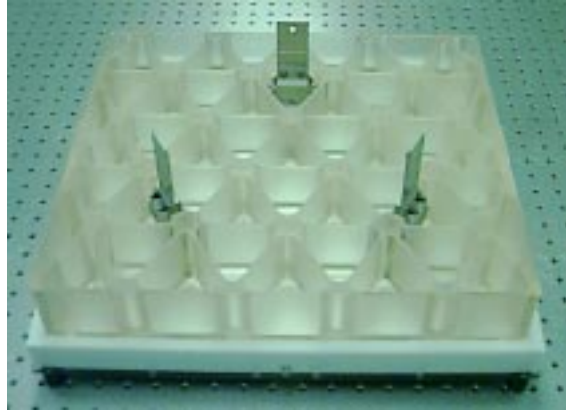


Figure 3. Photograph of a FUSE flight mirror resting on its face, showing lightweighting, titanium blade flexures, and Invar fittings (photo taken from the anti-vertex side).

ACKNOWLEDGMENTS

The authors gratefully acknowledge Jeff Hampton and Judy Yienger of Swales and Associates, Inc. for their help in testing and trouble shooting, Dan Vukobratovich of the National Optical Astronomy Observatories for his optomechanical support, and John Kincade and the rest of the FUSE team at Tinsley Laboratories, Inc. for their hard work and insight. This work is supported by NASA contract NAS5-32985.

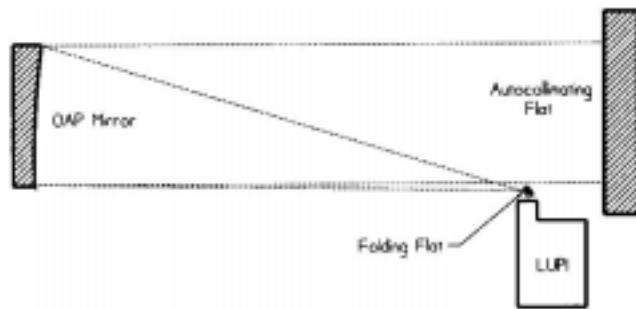
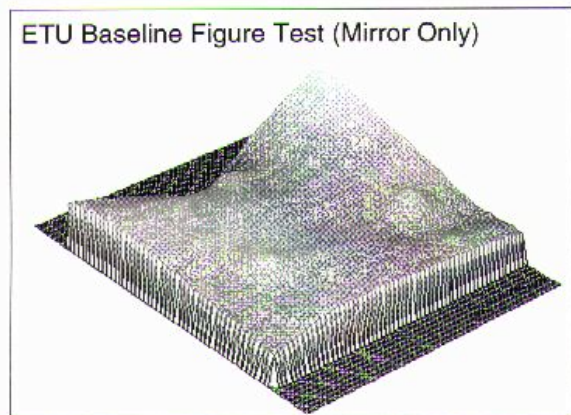
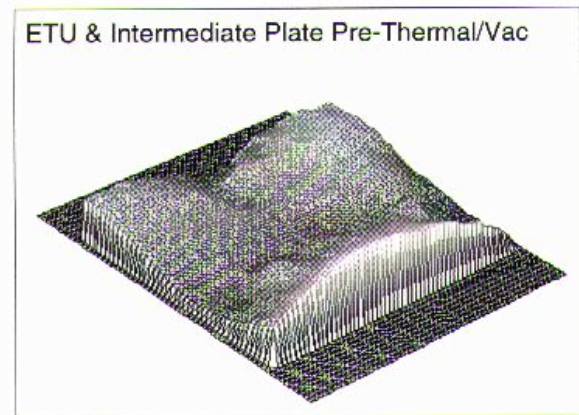


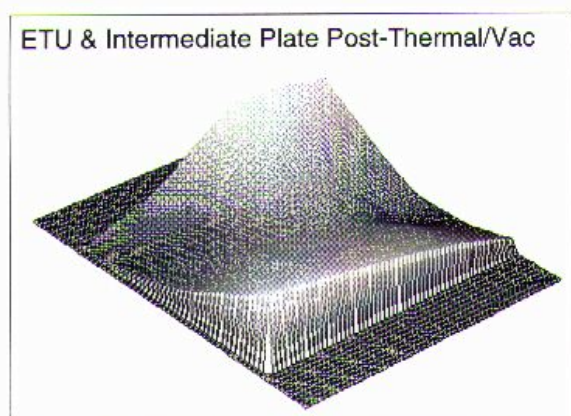
Figure 4. (a) Schematic drawing showing auto-collimating, interferometric figure test setup for off-axis parabolic flight mirrors (not to scale). (b) Photograph of flight mirror-plus-IP sub-assembly resting on metrology mount for figure test (photo taken from vertex side). Note vertex-side mirror support point on the bottom right above the dolly's front wheel and IP support spring above the IP in tension.



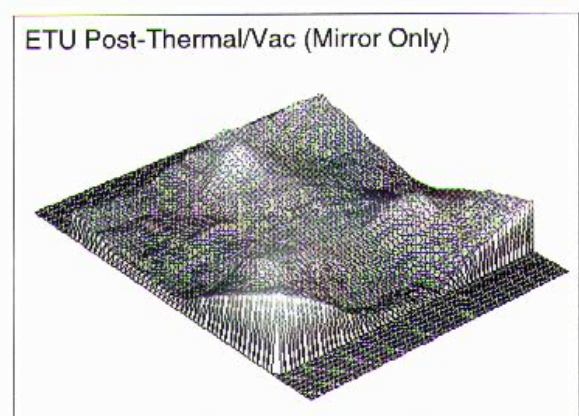
RMS: 0.034 wv P-V: 0.256 wv WL: 632.80 nm



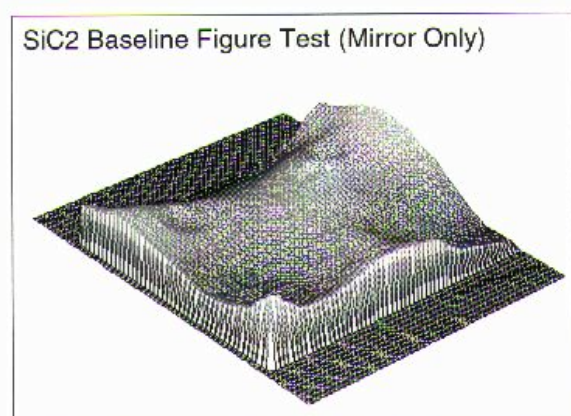
RMS: 0.049 wv P-V: 0.311 wv WL: 632.80 nm



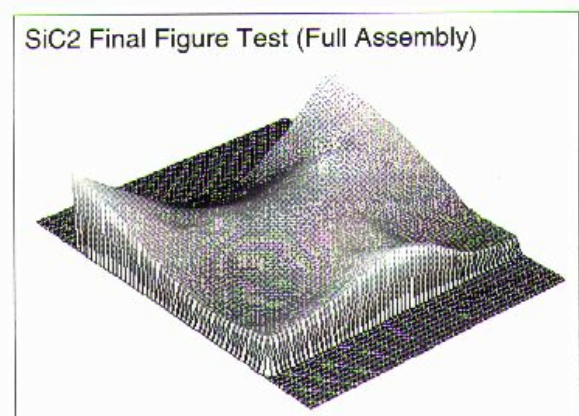
RMS: 0.300 wv P-V: 1.279 wv WL: 632.80 nm



RMS: 0.028 wv P-V: 0.182 wv WL: 632.80 nm



RMS: 0.026 wv P-V: 0.161 wv WL: 632.80 nm



RMS: 0.046 wv P-V: 0.263 wv WL: 632.80 nm

Figure 5. Figure test results. Each display has a different linear scale. For each surface, the RMS in “wavelengths” (wv) from the histogram of pixel values, the peak-to-valley (P-V), and the test wavelength are shown. (a) Initial figure test of ETU after delivery (post-flexure bonding). (b) ETU mirror-plus-IP sub-assembly figure test pre-TV. (c) ETU mirror-plus-IP sub-assembly figure test post-TV. (d) ETU figure test post-TV (mirror detached from hardware). (e) SiC 2 flight mirror figure test after delivery. (f) Final figure test of SiC 2 flight mirror, fully assembled and tested and ready for integration with the rest of the instrument.

REFERENCES

1. D. J. Sahnou, S. D. Friedman, H. W. Moos, J. C. Green, and O. H. W. Siegmund, Preliminary performance estimates for the *Far Ultraviolet Spectroscopic Explorer* (FUSE), *Proc. SPIE* **3356**, 1998 (this volume).
2. E. Wilkinson, J. C. Green, S. N. Osterman, K. R. Brownsberger, and D. J. Sahnou, Integration, alignment, and initial performance results of the *Far Ultraviolet Spectroscopic Explorer* (FUSE) spectrograph, *Proc. SPIE* **3356**, 1998 (this volume).
3. O. H. W. Siegmund, M. Gummin, J. Stock, G. Naletto, G. Gaines, R. Raffanti, J. Hull, R. Abiad, T. Rodriguez-Bell, T. Magoncelli, P. Jelinsky, W. Donakowski, and K. Kromer, Performance of the double delay line microchannel plate detectors for the Far Ultraviolet Spectroscopic Explorer, *Proc. SPIE* **3114**, pp. 283–294, 1997.
4. M. J. Kennedy, S. D. Friedman, R. H. Barkhouser, J. Hampton, and P. Nikulla, Design of the Far Ultraviolet Spectroscopic Explorer mirror assemblies, *Proc. SPIE* **2807**, pp. 172–183, 1996.
5. J. Harvey, “FUSE telescope performance predictions”, *unpublished report*, Center for Research and Education in Optics and Lasers, University of Central Florida, 1996.
6. J. Gum, Goddard Space Flight Center, private communication.
7. J. F. Osantowski, A. R. Toft, and R. S. Spencer, *unpublished report*, Goddard Space Flight Center, 1973.
8. M. Martinez, The Johns Hopkins University, private communication.
9. J. J. B. Houston, C. J. Buccini, and P. K. O’Neill, “A laser unequal path interferometer for the optical shop,” *Appl. Opt.* **6**, pp. 1237–1242, 1967.
10. D. Godfrey, The Dexter Corp., Dexter Aerospace Materials Division, private communication.
11. D. Vukobratavitch, National Optical Astronomy Observatories, private communication.
12. J. W. Pepi and D. Golini, “Delayed elasticity in zerodur at room temperature,” *Proc. SPIE* **1533**, pp. 212–221, 1991.